Natural and pretreated Gördes clinoptilolite for ammonia removal: Effect of the exchangeable cations (Na^+, K^+, Ca^{2+} and Mg^{2+})

Burcu Erdoğan[a]* and Orkun Ergürhan[a]

[a]*Department of Physics, Faculty of Science, Eskisehir Technical University, 26470 Eskisehir, Türkiye*

*Corresponding author:

e-mail: burcuerdogan@eskisehir.edu.tr

Tel: +90–222–2137907

Fax: +90–222–3204910

Mineralogical Society

This is a 'preproof' accepted article for Clay Minerals. This version may be subject to change during the production process.
DOI: 10.1180/clm.2024.5

Abstract

In this study, the effect of two different ammonium exchange methods to improve the ammonia (NH_3) gas adsorption of raw clinoptilolite (CLN) from Gördes (Türkiye) was investigated. The first method involved direct modification of CLN by 0.5 or 1.0 M NH_4NO_3 solutions at 80 °C for 4 and 8 h followed by calcination. In the second method, CLN was converted to the Na+ form prior to modification with ammonium nitrate and calcination under the same conditions. By both methods, H^+ forms of CLN were obtained through removal of exchangeable cations without damaging the crystal structure. Ammonia adsorption isotherms were determined at 298 K for total of eight different H+ forms synthetized by both methods. The Na-1.0-8h CLN sample with the highest ammonia adsorption capacity obtained by method 2 was selected as the parent CLN. In addition, in order to determine the effect of doping different cations into the structure on the NH_3 adsorption properties of the selected parent CLN sample, cation exchange processes were carried out using 0.5 and 1.0 M $NaNO_3$, KNO_3, $Ca(NO_3)_2$ and $Mg(NO_3)_2$ solutions at 80 °C for 4 h. The raw and modified clinoptilolites were characterized by XRD, XRF, SEM and N_2 adsorption analysis. Cation-exchanged samples with a wide range of ammonia adsorption capacity (3.61-4.93 $mmol.g^{-1}$) were compared with other zeolites in the literature.

https://doi.org/10.1180/clm.2024.5 Published online by Cambridge University Press

Keywords: Adsorption; Ammonia; BET; Clinoptilolite; XRD; XRF.

1. Introduction

The quality and chemistry of the Earth's atmosphere is critical to the future of human and mammalian life. Since the beginning of industrial activity, the chemical composition of the atmosphere has changed due to the release of volatile pollutants and greenhouse gases (Fowler, 2020). Ammonia (NH_3), an irritating, malodorous and colorless gas, is one of these pollutants. It is used as an ingredient in many commercial cleaning and pharmaceutical products, as a hydrogen carrier and as a fertilizer (Kobayashi, 2019; Sun et al., 2021) and for selective catalytic reduction of NO_x (Li et al., 2011; Wang et al., 2017). Large amounts of ammonia are released into the atmosphere by livestock farming and agricultural activities (Ciahotný, 2002). This ammonia release can be taken up by atmospheric moisture and surface water, as well as accumulation in plants and soil (Renard, 2004). Changes in atmospheric ammonia concentrations are known to have adverse effects on the environment (Amon, 1997). In addition, exposure to certain levels of ammonia can be extremely harmful to human health. Inhaled ammonia is mainly absorbed by water in human tissues, denaturing proteins and eventually destroying cell membranes (Sun et al., 2021). This can cause nausea, coughing, dizziness, pulmonary oedema and weakening of the immune system (Sun et al., 2021; Lindgren, 2010). Therefore, indoor

https://doi.org/10.1180/clm.2024.5 Published online by Cambridge University Press

ammonia concentrations can also pose a threat to the health of workers. For example, workers who work in an environment with high levels of ammonia are at risk of developing chronic respiratory diseases such as bronchial asthma (Ballal, 1998). Ammonia can also affect the reproductive function of female workers (Sun et al., 2021). Animals in livestock buildings are also affected by the presence of ammonia in the environment. One study shows that an inflammatory response is observed in the respiratory system of pigs exposed to ammonia concentrations of 100 and 150 ppm (Drummond, 1980). It is therefore clear that indoor ammonia levels also need to be controlled.

Many porous adsorbents such as metal–organic frameworks, covalent organic frameworks, hydrogen organic frameworks, porous organic polymers, and their composite materials have been studied in the literature for their ability to remove ammonia (Won Kang, 2020). One such adsorbent is zeolite, an alumina-silicate mineral found in nature or synthesized in the laboratory. The framework of a zeolite is formed by the combination of tetrahedral silicate $[SiO_4]^{4-}$ units. Combinations of these units form channels or networks. During the formation of zeolites, the isomorphic substitution of a trivalent cation such as Al^{3+} or $Ga^{3+}$for the Si^{4+} creates a negative charge that is balanced by the presence of exchangeable cations such as Na^{+}, Mg^{2+} and Ca^{2+}, etc. (Gottardi & Galli, 1985). Clinoptilolite, a natural zeolite, is a member of the heulandite (HEU) group. The general formula of clinoptilolite is $(Na,K)_6(Al_6Si_{30}O_{72})\cdot 20H_2O$. Its framework structure of monoclinic C_2/m

https://doi.org/10.1180/clm.2024.5 Published online by Cambridge University Press

symmetry with the unit cell parameters a = 17.62 Å, b = 17.91 Å, c = 7.39 Å and β = 116°16' is almost identical to that of heulandite. However, clinoptilolite has a higher Si/Al ratio (≥4) and is more thermally stable than heulandite (Mumpton, 1960; Ward & McKague 1994). Clinoptilolite has a 2-dimensional channel network (ten-membered A and eight-membered B channels run along the a-axis, while eight-membered C channels intersect them along the c-axis) (Ambrozova, 2017). In addition to its catalytic (Dziedzicka et al., 2016) and medical (Mastinu et al., 2019) applications, clinoptilolite is a preferred material for the removal of heavy metal ions (Zendelska et al., 2018; El-Arish et al., 2022; Elboughdiri, 2020), environmental pollutants from wastewater (Shamshiri et al., 2022), and toxic gases from air (Senila, 2022; Macala et al., 2009; A. Ghahri et al., 2017; Karousos et al., 2016).

It is common to apply the chemical processes such as treatment with acid (H_2SO_4, H_3PO_4 and HNO_3) and salt (KNO_3, $NaNO_3$ and $Mg(NO_3)_2$) solutions to improve the physicochemical and gas adsorption properties of the natural zeolites (Ciahotný et al., 2006; Erdoğan Alver & Sakızcı 2019). However, even at low molarities, dealumination during hydrochloric acid treatment causes the crystal structure to collapse rapidly (Garcia-Basabe et al., 2010). An alternative method to modify the structure of clinoptilolite is calcination after ammonium (NH_4^+) exchange. In this process, raw clinoptilolite is treated with ammonium salt solution and obtained product (or

https://doi.org/10.1180/clm.2024.5 Published online by Cambridge University Press

sample) was calcined at temperatures of 400-600 ºC for 2-8 h. In this way, ammonium ions adsorbed from the salt solution decompose into ammonia and hydrogen ions. As a result, H^+ forms of clinoptilolite with a higher surface area than the raw material can be obtained without damaging the structure (Allen et al., 2009; Rožić et al., (2005). In the literature, there are many studies in which H^+ forms of clinoptilolite were obtained using different calcination temperatures and various molarities of ammonium salt solutions (Kurama et al., 2002; Liao et al., 2019; Hieu et al., 2022; Elysabeth et al., 2019). However, it remains to be investigated how the ammonia adsorption properties of clinoptilolite in the H^+ form obtained after calcination change after modification with different cations. Therefore, the main objective of this study is to determine the ammonia adsorption capacity of H^+ forms synthesized by calcination after direct and indirect ammonium nitrate exchange and to select the most suitable parent sample in terms of ammonia retention. In a second step, the effect of doping the selected parent sample with K^+, Na^+, $Mg^{2+}$and Ca^{2+} cations on the ammonia adsorption efficiency was investigated.

2. Experimental

2.1. Materials and methods

Gördes clinoptilolite (CLN) was sieved with a sieving machine (Retsch, Germany) to obtain <125 µm fraction. To remove soluble impurities,

https://doi.org/10.1180/clm.2024.5 Published online by Cambridge University Press

each 5.0 g zeolite sample was kept in 100 ml deionized water at 80 ºC for 4 h. All samples were then separated and washed several times with hot distilled water. Two different methods were used to synthesize the samples (Fig. 1). In Method 1, where H^+ forms were obtained directly, the samples were modified with 100 ml of 0.5 and 1.0 M NH_4NO_3 solutions at 80 ºC for 4 and 8 h, respectively. The H^+ forms obtained by calcining these samples at 400°C for 6 h were labeled as 0.5-4h-CLN, 0.5-8h-CLN, 1.0-4h-CLN and 1.0-8h-CLN (Fig. 1).

In Method 2, where H^+ forms were obtained indirectly, clinoptilolite samples were first modified with 100 ml of 1.0 M NaNO3 solution at 80 oC for 4 hours. All samples were then separated and washed several times with hot distilled water and dried at room temperature. These samples were then modified with 100 ml of 0.5 and 1.0 M NH_4NO_3 solutions for 4 and 8 h and calcined at 400°C for 6 h to indirectly obtain H^+ forms. These samples were labeled as Na-0.5-4h-CLN, Na-0.5-8h-CLN, Na-1.0-4h-CLN, and Na-1.0-8h-CLN (Fig. 1). For all cation exchange procedures, 5.0 g of clinoptilolite sample was used per 100 ml of solution. Ammonia adsorption measurements of these eight different H^+-form clinoptilolite samples obtained by both methods were carried out at 298 K. Na-1.0-8h-CLN sample with the highest ammonia adsorption capacity among the H-forms (prepared by method 2) was selected as the main CLN (Table 2). In the second step after the selection of the parent sample, 5.0 g of each parent CLN sample was exchanged with 0.5

https://doi.org/10.1180/clm.2024.5 Published online by Cambridge University Press

and 1.0 M $NaNO_3$, KNO3, $Ca(NO_3)_2$ and $Mg(NO_3)_2$ solutions at 80 °C for 4 h to investigate the effect of doping the structure of this sample with different cations on the ammonia adsorption capacity. The cation exchanged samples of the parent sample were then separated and washed several times with deionized water at boiling point and the dried samples were then kept in an oven at 100 °C for 12 hours and stored in a desiccator. Finally, the cation exchanged samples of the parent sample are labeled as 0.5-Na-CLN, 0.5-K-CLN, 0.5-Ca-CLN, 0.5-Mg-CLN, 1.0-Na-CLN, 1.0-K-CLN, 1.0-Ca-CLN, 1.0 Mg-CLN depending on the salt solution used in cation exchange process.

2.2. Instrumentation

Raw and cation-exchanged clinoptilolite samples were characterized using X-ray fluorescence (XRF), X-ray diffraction (XRD), scanning electron microscopy (SEM) and N_2 adsorption techniques. Elemental analyses of the samples were performed using a Rigaku ZSX Primus instrument. Loss of ignition (LOI) was determined by mass measurement after the samples were heated to 1000°C at a heating rate of 10 °C/min, allowed to stand for 1 hour, and then cooled to room temperature at the same rate. Powder XRD diffractograms were obtained on a Bruker instrument (D8 Advance) using CuK_α (λ=1.54 Å) at 40 kV and 40 mA, in the range 5-40° of 2θ. Samples were scanned with a step of 0.02° of 2θ. SEM images were recorded with a Zeiss Ultra Plus field emission scanning electron microscope (FE-SEM) at 5 kV

https://doi.org/10.1180/clm.2024.5 Published online by Cambridge University Press

acceleration voltage. All samples were gold plated prior to analysis. Specific surface areas and micropore data were obtained from the nitrogen adsorption isotherms. Ammonia adsorption isotherms were measured at 298 K to 100 kPa for all samples. N_2 and NH_3 adsorption analyses of the clinoptilolites were performed using a 3Flex (Micromeritics) volumetric apparatus after degassing at 300 °C for 8 h.

3. Results and discussion

3.1. Elemental analysis

The results of XRF analysis of the raw CLN, parent CLN and that of cation exchanged forms (0.5-Na-CLN, 0.5-K-CLN, 0.5-Ca-CLN, 0.5-Mg-CLN, 1.0-Na-CLN, 1.0-K-CLN, 1.0-Ca-CLN and 1.0-Mg-CLN) are given in Table 1. Raw CLN is rich in potassium and calcium and has SiO_2/Al_2O_3 ratio of 5.7. Compared to the raw sample, the parent sample prepared using Method 2 was found to have significant changes in chemical composition and significant removal of exchangeable cations from the structure without damaging the crystal structure, as confirmed by XRD data. Prior to calcination, the cation exchange of available extra-framework cations (Na^+, K^+, Ca^{2+} and Mg^{2+}) with $NH4^+$ resulted in significant reductions in the chemical composition of the parent sample, especially in the CaO and K_2O components.

https://doi.org/10.1180/clm.2024.5 Published online by Cambridge University Press

As can be seen from Table 1, the chemical compositions of the cation-exchanged forms of the parent CLN were found to increase in their respective oxide compositions depending on the selected salt solution and the increasing molarity of this solution. Since the method 2 used to obtain the parent sample did not damage the crystal structure and did not cause dealumination, there was no significant change in the SiO_2/Al_2O_3 ratios of the parent sample and that of cation exchanged forms compared to the raw CLN.

3.2. XRD analysis

The powder XRD patterns obtained for the raw CLN, parent CLN, 0.5-Na-CLN, 0.5-K-CLN, 0.5-Ca-CLN, 0.5-Mg Na-CLN, 1.0-CLN, 1.0-K-CLN, 1.0-Ca-CLN, 1.0-Mg-CLN samples are shown in Fig. 2. The characteristic peaks of clinoptilolite for the CLN raw sample were observed at, d= 8.95, 7.91, 3.96 and 2.79 Å, corresponding to values of 2θ= 9.88°, 11.17°, 22.50° and 32.01°, with hkl indices (020), (200), (131) and (530), respectively (Moore & Renolds Jr., 1997). In addition to the clinoptilolite phase (80-85%), small amounts of feldspar (3%), opal-A (5-10%) and illite (2%) were also found in the raw CLN sample according to the method of Esenli and Sirkecioğlu, 2005. As can be seen from Fig. 2, the position of the main clinoptilolite peaks has not changed significantly for the parent CLN and that of the cation-exchanged forms. Compared to raw CLN, the relative peak intensity of (200) for the parent CLN and other cation exchanged forms

https://doi.org/10.1180/clm.2024.5 Published online by Cambridge University Press

was found to decrease compared to the peak intensity of (020), except for the 0.5-K-CLN and 1.0-K-CLN samples. The changes in the absolute and relative intensities of the characteristic peaks of the clinoptilolite samples can be attributed to the changes in the atomic positions and atomic density in the structure and in the pore size and pore shape of the clinoptilolite (Rodríguez-Iznaga et al., 2022; Kennedy & Tezel, 2018; Castaldi et al., 2008; Galli et al., 1983). The relative changes in peak intensities in our XRD results can be attributed to changes in the exchangeable cation ratios as shown in the XRF data (Table 1), since the intensity of the (020) peak is highly dependent on the Na/K ratio of the clinoptilolite samples (Kitsopoulost, 2001). Furthermore, the absence of a broad baseline between 19° and 30° 2θ for the major CLN and cation exchanged forms indicates that the method used in this study does not damage the clinoptilolite structure, unlike other modification methods such as acid modification (Garcia-Basabe et al., 2010; Kennedy & Tezel, 2018; Arcoya et al., 1994).

The unit cell parameters (a, b, c and β) and volumes of the clinoptilolite samples obtained from the h, k and l dimensions in the monoclinic crystal structure are given in Table 2. It was found that there was a decrease in the unit cell volume value of the parent sample compared to the raw sample. This decrease due to calcination is similar to the results of other studies on clinoptilolite (Kudoh et al., 1983; Bish, 1984; Tomazović et al, 1996[a]; Tomazović et al, 1996[b]. In addition, the unit cell volume values of all

https://doi.org/10.1180/clm.2024.5 Published online by Cambridge University Press

cation-doped forms were found to be larger than the unit cell volume of the parent sample.

3.3. SEM

The SEM images taken at a magnification of at 5kX and 14kx for raw CLN, parent CLN, 0.5-Na-CLN, 0.5-K-CLN, 0.5-Ca-CLN, 0.5-Mg-CLN, 1.0-Na-CLN, 1.0-K-CLN, 1.0-Ca-CLN and 1.0-Mg-CLN samples are shown in Figs. 3 and 4. As shown in Figs. 3 and 4. (a)-(e), euhedral and subhedral plates, as well as coffin-shaped forms, were observed in all samples (Favvas et al., 2016; Brundu & Cerri 2015). HEU type crystals can be seen as platy, tabular or coffin shaped geometries (Elaiopoulos et al., 2010). In addition, some submicron and irregularly shaped clinoptilolite grains are also seen in all micrographs. The size of the crystals is consistent with the mineral obtained from the same region (Ünaldi et al., 2013). These results are consistent with similar studies (Favvas et al., 2016; Fajdek-Bieda et al., 2021).

3.4. Adsorption of nitrogen (N_2)

Figs. 5 and 6 show all the N_2 adsorption isotherms measured at 77 K. The specific surface areas, the micropore areas and micropore volumes of all the samples were determined by the BET and the t-plot methods, respectively (Table 3). All isotherms are type II according to IUPAC (Lowell et al., 2004). The knee portion of the isotherm shows the stage when the coverage of the

https://doi.org/10.1180/clm.2024.5 Published online by Cambridge University Press

monolayer is complete, and the multilayer adsorption begins to take place (Helminen et al., 2001; Lowell et al., 2004). The parent CLN was found to have higher values for specific surface area (106.93 $m^2.g^{-1}$), micropore area (81.27 $m^2.g^{-1}$) and micropore volume (0.0317 $cm^3.g^{-1}$) values compared to those of the raw CLN sample (Table 3). This can be explained by the removal of exchangeable cations (K^+, Na^+, Mg^{2+} and Ca^{2+}) from the structure by the method used in the study, the preservation of the H^+ form without damaging the crystal structure, and the easier diffusion of nitrogen. Similar increases in the BET values have been found for the NH_4NO_3 exchanged clinoptilolite from Germany (Hieu et al., 2022) and the NH_4Cl exchanged clinoptilolite from Bigadic (Kurama et al., 2002). In addition, the BET surface areas of cation-exchanged samples showed a wide variation in the range of 30.72-198.98 $m^2.g^{-1}$. The maximum specific surface area of the 1.0-Mg-CLN sample can be explained by the replacement of exchangeable cations such as Ca^{2+} and K^+ by Mg^{2+} (smaller in size), as confirmed by the XRF data (Table 1).

3.5. Adsorption of ammonia (NH_3)

Direct or indirect ion exchange with NH_4NO_3 followed by calcination method is applied to zeolite-type materials because it allows the removal of exchangeable cations in the structure and the structure to be uniform, unlike the methods of treating them with acid solutions such as HCl or H_2SO_4,

https://doi.org/10.1180/clm.2024.5 Published online by Cambridge University Press

without damaging the crystal structure. In this study, the direct and indirect ammonium nitrate treatment methods before calcination were carried out using multiple molarities (0.5 and 1.0 M). The 0.5-4h-CLN (3.95 $mmol.g^{-1}$), 0.5-8h-CLN (4.02 $mmol.g^{-1}$), 1.0-4h-CLN (3.99 $mmol.g^{-1}$) and 1.0-8h-CLN (3.92 $mmol.g^{-1}$) samples in which the H^+ forms were obtained directly without conversion to the Na^+ form, defined as method 1, adsorbed less ammonia than the other Na-0.5-4h-CLN (4.19 $mmol.g^{-1}$), Na-0.5-8h-CLN (4.07 $mmol.g^{-1}$), Na-1.0-4h-CLN (4.10 $mmol.g^{-1}$) and Na-1.0-8h-CLN (4.46 $mmol.g^{-1}$) samples obtained by method 2. In these H^+ forms obtained by these two methods, the removal of exchangeable cations such as Mg^{2+}, Ca^{2+} and Na^+ in the structure by direct or indirect ion exchange with NH_4NO_3 followed by calcination caused a general decrease in the ammonia adsorption capacities compared to the raw sample. For this reason, Na-1.0-8h, which has the highest ammonia adsorption capacity among the H^+ forms, was selected as the parent sample. The next step was to determine the ammonia adsorption capacities by doping the parent sample with different cations. The ammonia adsorption isotherms of the raw CLN, the parent sample and that of cation exchanged forms at 298 K up to a pressure of 100 kPa are shown in Figs. 7 and 8.

The ammonia uptake of the clinoptilolite samples ranged from 3.61 to 4.93 $mmol.g^{-1}$ and increased in the following order: 1.0-K-CLN < 0.5-K-CLN < 1.0-Mg-CLN < 1.0-Na-CLN < 0.5-Mg-CLN < raw CLN < parent CLN < 1.0-Ca-CLN < 0.5-Ca-CLN < 0.5-Na-CLN (Table 4). When the molarity of

https://doi.org/10.1180/clm.2024.5 Published online by Cambridge University Press

the salt solutions used was twice higher (from 0.5 M to 1.0 M), the ammonia adsorption capacity decreased. The raw CLN sample showed lower ammonia uptake (4.41 $mmol.g^{-1}$) compared to clinoptilolite from Mud Hills, USA (5.90 $mmol.g^{-1}$) (Helminen et al., 2001), but higher than Slovakian clinoptilolite (0.71 $mmol.g^{-1}$) (Ciahotný et al., 2006), due to its different mineralogical and chemical composition. Although the specific surface area (106.93 m^2.g-1) and micropore surface area (81.27 $m^2.g^{-1}$) values of the parent CLN were higher than those of the cation exchanged forms (30.72-93.15 $m^2.g^{-1}$) and (8.46-67.75 $m^2.g^{-1}$) with 0.5 and 1.0 M $NaNO_3$, KNO_3 and $Ca(NO_3)_2$ solutions, respectively (Table 4), it showed an average ammonia adsorption capacity. This can be attributed to the significant removal of exchangeable cations in the parent sample, one of the H-forms obtained using method 2. This also clearly demonstrates the influence of the extra framework cations on ammonia adsorption and the interactions of the permanent dipole moment (1.47 Debye) of the ammonia molecule with the electric field generated by these cations. Among the cation modified forms of the parent sample, 0.5-Na-CLN (4.93 $mmol.g^{-1}$) showed the highest uptake. This result for the 0.5-Na-CLN sample showed that it is beneficial to doping the parent sample with Na^+ cation in a second step. As shown in Fig. 9, in clinoptilolite, Na^+, Ca^{2+}, and K^+ cations prefer to occupy sites the M(1) (in channel A), M(2) (in channel B), and M(3) (in channel C), respectively, while the Mg^{2+} cation is located at the site M(4) (in channel A) (Koyama & Takeuchi, (1977). The

https://doi.org/10.1180/clm.2024.5 Published online by Cambridge University Press

exchange of Na^+ with the Mg^{2+}, Ca^{2+} and K^+ cations and the presence of this smallest size cation in the M(1) site of channel A led to a larger space within the channels. On the other hand, the 1.0 K-CLN sample was found to have both the lowest specific surface area (30.72 $m^2.g^{-1}$) and the lowest ammonia adsorption capacity (3.61 $mmol.g^{-1}$) due to the size and position of the K^+ (largest) cation and partial pore blocking. The % change of ammonia adsorption capacity of parent and cation exchanged forms compared to the natural sample was found to be in the range of 0.45 to 18.14.

As shown in Table 4, the ammonia adsorption capacity of the 0.5-Na-CLN sample (4.93 $mmol.g^{-1}$) is lower than that of MOF-177 (12.2 $mmol.g^{-1}$) (Saha & Deng[a], 2010), 13X (9.33 $mmol.g^{-1}$) (Helminen et al., 2001), 4A (8.71 $mmol.g^{-1}$) (Helminen et al., 2001) and mesoporous carbon (6.39 $mmol.g^{-1}$) (Saha, & Deng[b], 2010), but higher than those of activated alumina (2.53 $mmol.g^{-1}$) (Saha, & Deng[c], 2010), pentasil dealuminated (2.34 $mmol.g^{-1}$) [51], activated carbon (4.19 $mmol.g^{-1}$) (Helminen et al., 2001), faujasite dealuminated (1.77 $mmol.g^{-1}$) (Helminen et al., 2001) and Cu-MOF-74 (3.4 $mmol.g^{-1}$) (Katz et al., 2016). Comparing the ammonia adsorption data obtained at the same temperature in Table 4, it is clear that the structural and textural properties of these synthetic materials are completely different from natural zeolite of clinoptilolite type. Although synthetic zeolites, due to their uniform structure, generally have higher gas adsorption capacities than natural zeolites, they are more expensive. The abundance of clinoptilolite type

https://doi.org/10.1180/clm.2024.5 Published online by Cambridge University Press

natural zeolite, its low cost, and its high capacity to adsorb harmful gases such as ammonia lead to its widespread use in industrial applications. As a result, 0.5-Na-CLN sample with the highest ammonia adsorption capacity can be recommended as an effective adsorbent in environments where ammonia gas needs to be removed, such as poultry houses.

4. Conclusions

In this study, the structural properties and ammonia adsorption capacities of the parent CLN and its forms doped with Na^+, K^+, Ca^{2+} and Mg^{2+} cations were compared. The XRD data of the clinoptilolite samples showed that the NH_4NO_3 modification and the calcination process to obtain the H^+ forms prior to the cation exchange did not cause any significant damage to the crystal structure. It was also found that the morphology of the modified samples was not affected by calcining. A more than threefold increase in BET surface area (106.93 $m^2.g^{-1}$) was observed for the parent sample compared to the raw CLN (30.08 $m^2.g^{-1}$). Clinoptilolite samples in which the H^+ forms were obtained by first converting to the Na^+ form (as a result of ammonium nitrate and calcination), as defined by method 2, adsorbed more ammonia than directly obtained H^+ forms, as defined by method 1. A wide variation in ammonia adsorption was observed in the cation exchanged clinoptilolites depending more on the size, amount and location of the exchanged cation rather than on the BET surface areas. Consequently, 0.5-Na-CLN, which has

https://doi.org/10.1180/clm.2024.5 Published online by Cambridge University Press

the highest ammonia adsorption capacity among the samples used in this study, can be suggested as a potential material for ammonia removal applications.

Acknowledgments

Financial support from Eskisehir Technical University Scientific Research Committee under grant number 22ADP355 is gratefully acknowledged. The authors also thank Ceramic Research Center (SAM, Eskisehir/Turkey) for XRF analysis of all samples.

https://doi.org/10.1180/clm.2024.5 Published online by Cambridge University Press

References

Allen S.J., Ivanova E. & Koumanova B. (2009) Adsorption of sulfur dioxide on chemically modified natural clinoptilolite. Acid modification. *Chemical Engineering Journal*, **152** 389–395. https://doi.org/10.1016/j.cej.2009.04.063.

Ambrozova P., Kynicky J., Urubek T. & Nguyen V.D. (2017) Synthesis and modification of clinoptilolite. *Molecules*, **22** Page 1107. https://doi.org/10.3390/MOLECULES22071107.

Amon M., Dobeic M., Sneath R.W., Phillips V.R., Misselbrook T.H. & Pain B.F. (1997) A farm-scale study on the use of clinoptilolite zeolite and De-Odorase® for reducing odour and ammonia emissions from broiler houses. *Bioresource Technology*, **61** 229–237. https://doi.org/10.1016/S0960-8524(97)00005-9.

Arcoya A., González J.A., Travieso N. & Seoane X.L. Physicochemical and catalytic properties of a modified natural clinoptilolite. *Clay Minerals*, **29** (1994) 123–131. https://doi.org/10.1180/claymin.1994.029.1.14.

Ballal S.G., Ali B.A., Albar A.A., Ahmed H.O. & Al-Hasan A.Y. (1998) Bronchial asthma in two chemical fertilizer producing factories in eastern Saudi Arabia. *The International Journal of Tuberculosis and Lung Disease*, **2** 330–335.

https://doi.org/10.1180/clm.2024.5 Published online by Cambridge University Press

Bish D.L. (1984) Effects of Exchangeable cation composition on the thermal expansion/contraction of clinoptilolite. *Clays and Clay Minerals*, **32** 444–452. https://doi.org/10.1346/CCMN.1984.0320602.

Brundu A., & Cerri G. (2015) Thermal transformation of Cs-clinoptilolite to $CsAlSi_5O_{12}$. Microporous and Mesoporous Materials, 208, 44-49. https://doi.org/10.1016/j.micromeso.2015.01.029.

Castaldi P., Santona L., Enzo S. & Melis P. (2008) Sorption processes and XRD analysis of a natural zeolite exchanged with Pb^{2+}, Cd^{2+} and Zn^{2+} cations. *Journal of Hazardous Materials*, **156** 428–434. https://doi.org/10.1016/j.jhazmat.2007.12.040.

Ciahotný K., Melenová L., Jirglová H., Boldiš M. & Kočiřík M. (2002) Sorption of ammonia from gas streams on clinoptilolite impregnated with inorganic acids. *Studies in Surface Science and Catalysis*, **142 B** 1713–1720. https://doi.org/10.1016/S0167-2991(02)80344-5.

Ciahotný K., Melenová L., Jirglová H., Pachtová O., Kočiřík M. & Eić M. (2006) Removal of ammonia from waste air streams with clinoptilolite tuff in its natural and treated forms. *Adsorption*, **12** 219–226. https://doi.org/10.1007/s10450-006-0148-x.

Drummond J.G., Curtis S.E., Simon J. & Norton H.W. (1980) Effects of aerial ammonia on growth and health of young pigs. *Journal of Animal Science*, **50** 1085–1091. https://doi.org/10.2527/JAS1980.5061085X.

https://doi.org/10.1180/clm.2024.5 Published online by Cambridge University Press

Dziedzicka A., Sulikowski B. & Ruggiero-Mikołajczyk M. (2016) Catalytic and physicochemical properties of modified natural clinoptilolite, *Catalysis Today*, **259** 50–58. https://doi.org/10.1016/J.CATTOD.2015.04.039.

El-Arish N.A.S., Zaki R.S.R.M., Miskan S.N., Setiabudi H.D. & Jaafar N.F. (2022) Adsorption of Pb(II) from aqueous solution using alkaline-treated natural zeolite: Process optimization analysis. *Total Environment Research Themes*, **3–4** 100015. https://doi.org/10.1016/j.totert.2022.100015.

Elaiopoulos K., Perraki T. & Grigoropoulou E. (2010) Monitoring the effect of hydrothermal treatments on the structure of a natural zeolite through a combined XRD, FTIR, XRF, SEM and N_2-porosimetry analysis. *Microporous and Mesoporous Materials*, **134** 29–43. https://doi.org/10.1016/J.MICROMESO.2010.05.004.

Elboughdiri. N. (2020) The use of natural zeolite to remove heavy metals Cu (II), Pb (II) and Cd (II), from industrial wastewater. *Cogent Engineering*, **7** 1782623. https://doi.org/10.1080/23311916.2020.1782623.

Elysabeth T., Zulnovri, Ramayanti G., Setiadi S. & Slamet S. (2019) Modification of Lampung and Bayah natural zeolite to enhance the efficiency of removal of ammonia from wastewater. *Asian Journal of Chemistry*, **31** 873–878. https://doi.org/10.14233/ajchem.2019.21810.

Erdoğan Alver B. & Sakızcı M. (2019) Hydrogen (H_2) adsorption on natural and cation-exchanged clinoptilolite, mordenite and chabazite. *International*

https://doi.org/10.1180/clm.2024.5 Published online by Cambridge University Press

Journal of Hydrogen Energy, **44** 6748-6755. https://doi.org/10.1016/j.ijhydene.2019.01.203

Esenli F. & Sirkecioğlu A. (2005) The relationship between zeolite (heulandite-clinoptilolite) content and the ammonium-exchange capacity of pyroclastic rocks in Gördes, Turkey. *Clay Minerals*, **40** 557–564. https://doi.org/10.1180/0009855054040192.

Fajdek-Bieda A., Wróblewska A., Miądlicki P., Tołpa J. & Michalkiewicz B. (2021) Clinoptilolite as a natural, active zeolite catalyst for the chemical transformations of geraniol. *Reaction Kinetics, Mechanisms and Catalysis*, **133** 997–1011. https://doi.org/10.1007/S11144-021-02027-3/FIGURES/8.

Favvas E.P., Tsanaktsidis C.G., Sapalidis A.A., Tzilantonis G.T., Papageorgiou S.K. & Mitropoulos A.C. (2016) Clinoptilolite, a natural zeolite material: Structural characterization and performance evaluation on its dehydration properties of hydrocarbon-based fuels. *Microporous and Mesoporous Materials*, **225** 385–391. https://doi.org/10.1016/J.MICROMESO.2016.01.021.

Fowler D., Brimblecombe P., Burrows J., Heal M.R., Grennfelt P., Stevenson, D.S., Jowett A., Nemitz E., Coyle M., Lui X., Chang Y., Fuller G.W., Sutton M.A., Klimont Z., Unsworth M.H. & Vieno M. (2020) A chronology of global air quality. *Philosophical Transactions of the Royal Society A*, **378** https://doi.org/10.1098/RSTA.2019.0314.

https://doi.org/10.1180/clm.2024.5 Published online by Cambridge University Press

Galli E., Gottardi G., Mayer H., Preisinger A. & Passaglia E. (1983) The structure of potassium-exchanged heulandite at 293, 373 and 593 K. *Acta Crystallographica Section B*, **39** 189–197. https://doi.org/10.1107/S010876818300227X.

Garcia-Basabe Y., Rodriguez-Iznaga I., Menorval L.C. De, Llewellyn P., Maurin G., Lewis D.W., Binions R., Autie M. & Ruiz-Salvador A.R. (2010) Step-wise dealumination of natural clinoptilolite: Structural and physicochemical characterization. *Microporous and Mesoporous Materials*, **135** 187–196. https://doi.org/10.1016/j.micromeso.2010.07.008.

Ghahri A., Golbabaei F., Vafajoo L., Mireskandari S.M., Yaseri M. & Shahtaheri S.J. (2017) Removal of greenhouse gas (N_2O) by catalytic decomposition on natural clinoptilolite zeolites impregnated with cobalt, *International Journal of Environmental Research*, **11** 327–337. https://doi.org/10.1007/s41742-017-0030-6.

Gottardi G. & Galli E. (1985) *Natural Zeolites*, Springer Berlin Heidelberg, Berlin, Heidelberg. https://doi.org/10.1007/978-3-642-46518-5.

Helminen J., Helenius J., Paatero E. & Turunen I. (2001) Adsorption equilibria of ammonia gas on inorganic and organic sorbents at 298.15 K, *Journal of Chemical Engineering Data*, **46** 391–399. https://doi.org/10.1021/je000273+.

Hieu D.T., Kosslick H., Riaz M., Schulz A., Springer A., Frank M., Jaeger C., Thu N.T.M. & Son L.T. (2022) Acidity and stability of Brønsted acid sites

https://doi.org/10.1180/clm.2024.5 Published online by Cambridge University Press

in green clinoptilolite catalysts and catalytic performance in the etherification of glycerol. Catalysts, **12** 253. https://doi.org/10.3390/catal12030253.

Karousos D.S., Sapalidis A.A., Kouvelos E.P., Romanos G.Em. & Kanellopoulos N.K. (2016) A study on natural clinoptilolite for CO_2 /N_2 gas separation. *Separation Science and Technology*, **51** 83–95. https://doi.org/10.1080/01496395.2015.1085880.

Katz M.J., Howarth A.J., Moghadam P.Z., DeCoste J.B., Snurr R.Q., Hupp J.T. & Farha O.K. (2016) High volumetric uptake of ammonia using Cu-MOF-74/Cu-CPO-27. Dalton Transactions, **45** 4150–4153. https://doi.org/10.1039/C5DT03436A.

Kennedy D.A. & Tezel, F.H. (2018) Cation exchange modification of clinoptilolite – Screening analysis for potential equilibrium and kinetic adsorption separations involving methane, nitrogen, and carbon dioxide. *Microporous and Mesoporous Materials*, **262** 235–250. https://doi.org/10.1016/j.micromeso.2017.11.054.

Kitsopoulost K.P. (2001) The relationship between the thermal behavior of clinoptilolite and its chemical composition. *Clays and Clay Minerals*, **49** 236-243. https://doi.org/10.1346/CCMN.2001.0490306

Kobayashi H., Hayakawa A., Somarathne K.D.K.A. & Okafor E.C. (2019) Science and technology of ammonia combustion. *Proceedings of the Combustion Institute*, **37** 109–133. https://doi.org/10.1016/J.PROCI.2018.09.029.

https://doi.org/10.1180/clm.2024.5 Published online by Cambridge University Press

Koyama K. & Takeuchi Y. (1977) Clinoptilolite: the distribution of potassium atoms and its role in thermal stability. *Zeitschrift Für Kristallographie-Crystalline Materials*, **145** 216–239.

Kudoh Y. & Takéuchi Y. (1983) Thermal stability of clinoptilolite: The crystal structure at 350 °C. *Mineralogical Journal*, **11** 392–406. https://doi.org/10.2465/minerj.11.392.

Kurama H., Zimmer A. & Reschetilowski W. (2002) Chemical Modification Effect on the Sorption Capacities of Natural Clinoptilolite. *Chemical Engineering & Technology*, **25** 301–305. https://doi.org/10.1002/1521-4125(200203)25:3<301::AID-CEAT301>3.0.CO;2.

Li J., Chang H., Ma L., Hao J. & Yang R.T. (2011) Low-temperature selective catalytic reduction of NOx with NH_3 over metal oxide and zeolite catalysts—A review. *Catalysis Today*, **175** 147–156. https://doi.org/10.1016/j.cattod.2011.03.034.

Liao J., Zhang Y., Fan L., Chang L. & Bao W. (2019) Insight into the acid sites over modified nay zeolite and their adsorption mechanisms for thiophene and benzene. Industrial & Engineering Chemistry Research, **58** 4572–4580. https://doi.org/10.1021/acs.iecr.8b05046.

Lindgren T. (2010) A case of indoor air pollution of ammonia emitted from concrete in a newly built office in Beijing. *Building and Environment*, **45** 596–600. https://doi.org/10.1016/J.BUILDENV.2009.07.014.

https://doi.org/10.1180/clm.2024.5 Published online by Cambridge University Press

Lowell S., Shields J.E., Thomas M.A. & Thommes M. (2004) Characterization of Porous Solids and Powders: Surface Area, Pore Size and Density, Kluwer Academic Publishers, Dordrecht, Netherlands.

Macala J., Pandova I., & Panda A. (2009) Clinoptilolite as a mineral usable for cleaning of exhaust gases. *Gospodarka Surowcami Mineralnymi*, **25** 23-32.

Mastinu A., Kumar A., Maccarinelli G., Bonini S.A., Premoli M., Aria F., Gianoncelli A. & Memo M. (2019) Zeolite clinoptilolite: therapeutic virtues of an ancient mineral, *Molecules*, **24** 1517. https://doi.org/10.3390/MOLECULES24081517.

Moore D.M. & Renolds Jr. R.C. (1997) X-ray diffraction and the identification and analysis of clay minerals., 2nd ed., Oxford University Press, New York.

Mumpton, F.A. (1960) Clinoptilolite redefined. *American Minerologist,* **45** 351–369.

Rodríguez-Iznaga I., Shelyapina M.G. & Petranovskii V. (2022) Ion exchange in natural clinoptilolite: aspects related to its structure and applications. *Minerals*, **12** 1628. https://doi.org/10.3390/min12121628.

Rožić, M. Cerjan-Stefanović Š., Kurajica S., Maěefat M.R., Margeta K. & Farkaš A. (2005) Decationization and dealumination of clinoptilolite tuff and ammonium exchange on acid-modified tuff. *Journal of Colloid and Interface Science*, **284** 48–56. https://doi.org/10.1016/j.jcis.2004.09.061.

https://doi.org/10.1180/clm.2024.5 Published online by Cambridge University Press

[a]Saha D. & Deng S. (2010) Ammonia adsorption and its effects on framework stability of MOF-5 and MOF-177. *Journal of Colloid and Interface Science*, 348 615–620. https://doi.org/10.1016/j.jcis.2010.04.078.

[b]Saha D. & Deng S. (2010) Adsorption equilibrium and kinetics of CO_2, CH_4, N_2O, and NH_3 on ordered mesoporous carbon. *Journal of Colloid and Interface Science*, **345** 402–409. https://doi.org/10.1016/j.jcis.2010.01.076.

[c]Saha D. & Deng S. (2010) Characteristics of ammonia adsorption on activated alumina. Journal of Chemical Engineering Data, **55** 5587–5593. https://doi.org/10.1021/je100405k.

Senila M., Neag E., Cadar O., Hoaghia M.A., Roman M., Moldovan A., Hosu A., Lupas A. & Kovacs E.D. (2022) Characteristics of volcanic tuff from Macicasu (Romania) and its capacity to remove ammonia from contaminated air. *Molecules*, **27** 3503. https://doi.org/10.3390/MOLECULES27113503.

Shamshiri A., Alimohammadi V., Sedighi M., Jabbari E. & Mohammadi M. (2022) Enhanced removal of phosphate and nitrate from aqueous solution using novel modified natural clinoptilolite nanoparticles: process optimization and assessment. *International Journal of Environmental Analytical Chemistry*, **102** 5994–6013. https://doi.org/10.1080/03067319.2020.1807525.

Sun C., Hong S., Cai G., Zhang Y., Kan H., Zhao Z., Deng F., Zhao B., Zeng X., Sun Y., Qian H., Liu W., Mo J., Guo J., Zheng X., Su C., Zou Z., Li H. &

https://doi.org/10.1180/clm.2024.5 Published online by Cambridge University Press

Huang C. (2021) Indoor exposure levels of ammonia in residences, schools, and offices in China from 1980 to 2019: A systematic review. *Indoor Air*, **31** 1691–1706. https://doi.org/10.1111/INA.12864.

Renard J.J., Calidonna S.E. & Henley M.V. (2004) Fate of ammonia in the atmosphere—a review for applicability to hazardous releases. *Journal of Hazardous Materials*, **108** 29–60. https://doi.org/10.1016/J.JHAZMAT.2004.01.015.

[a]Tomazović B., Ćeranić T. & Sijarić G. (1996) The properties of the NH_4-clinoptilolite. Part 1. Zeolites, **16** 301–308. https://doi.org/10.1016/0144-2449(95)00118-2.

[b]Tomazović B., Ćeranić T. & Sijarić G. (1996) The properties of the NH_4-clinoptilolite. Part 2. Zeolites, **16** 309–312. https://doi.org/10.1016/0144-2449(95)00117-4.

Ünaldi T., Mizrak I. & Kadir S. (2013) Physicochemical characterisation of natural K-clinoptilolite and heavy-metal forms from Gördes (Manisa, western Turkey). *Journal of Molecular Structure*, **1054–1055** 349–358. https://doi.org/10.1016/J.MOLSTRUC.2013.09.048.

Ward R.L. & McKague H.L. (1994) Clinoptilolite and heulandite structural differences as revealed by multinuclear nuclear magnetic resonance spectroscopy. *Journal of Physical Chemistry*, **98** 1232–1237. https://doi.org/10.1021/J100055A031/ASSET/J100055A031.FP.PNG_V03.

https://doi.org/10.1180/clm.2024.5 Published online by Cambridge University Press

Wang J., Zhao H., Haller G. & Li Y. (2017) Recent advances in the selective catalytic reduction of NOx with NH_3 on Cu-Chabazite catalysts. Applied Catalysis B, **202** 346–354. https://doi.org/10.1016/j.apcatb.2016.09.024.

Won Kang D., Eungyung Ju S., Won Kim D., Kang M., Kim H. & Seop Hong C. (2020) Emerging porous materials and their composites for NH_3 gas removal. *Advanced Science*, **7** 2002142. https://doi.org/10.1002/advs.202002142.

Zendelska A., Golomeova M., Jakupi Š., Lisičkov K., Kuvendžiev S. & Marinkovski M. (2018) Characterization and application of clinoptilolite for removal of heavy metal ions from water resources. *Geologica Macedonica*, **32** 21–32.

https://doi.org/10.1180/clm.2024.5 Published online by Cambridge University Press

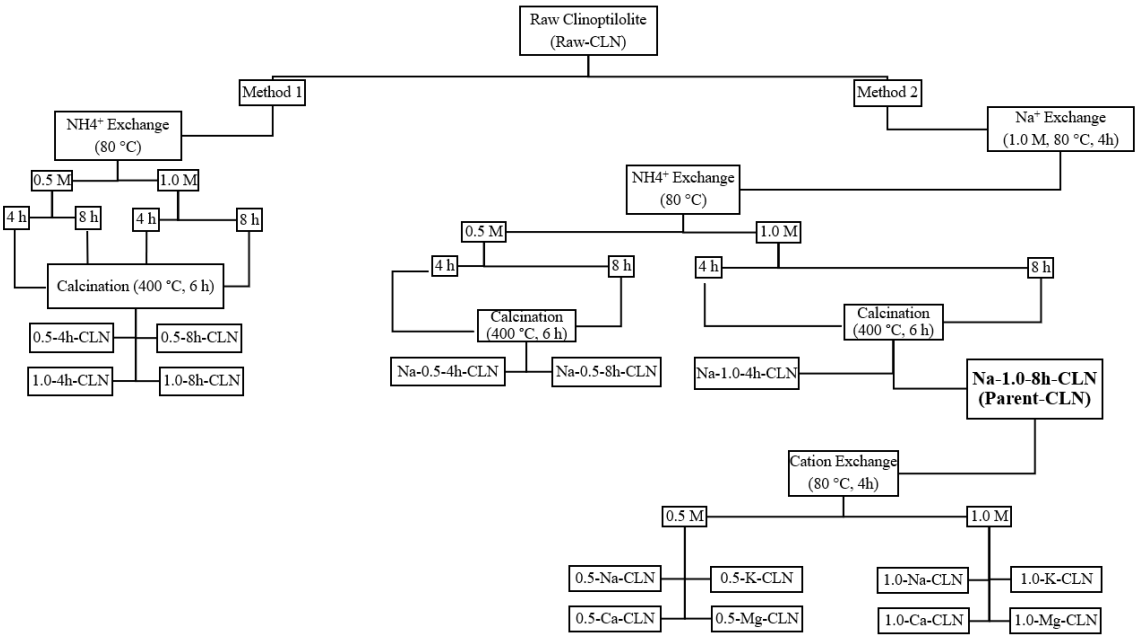

Fig. 1. Schema of the sample preparation procedure.

Mineralogical Society

This is a 'preproof' accepted article for Clay Minerals. This version may be subject to change during the production process.
DOI: 10.1180/clm.2024.5

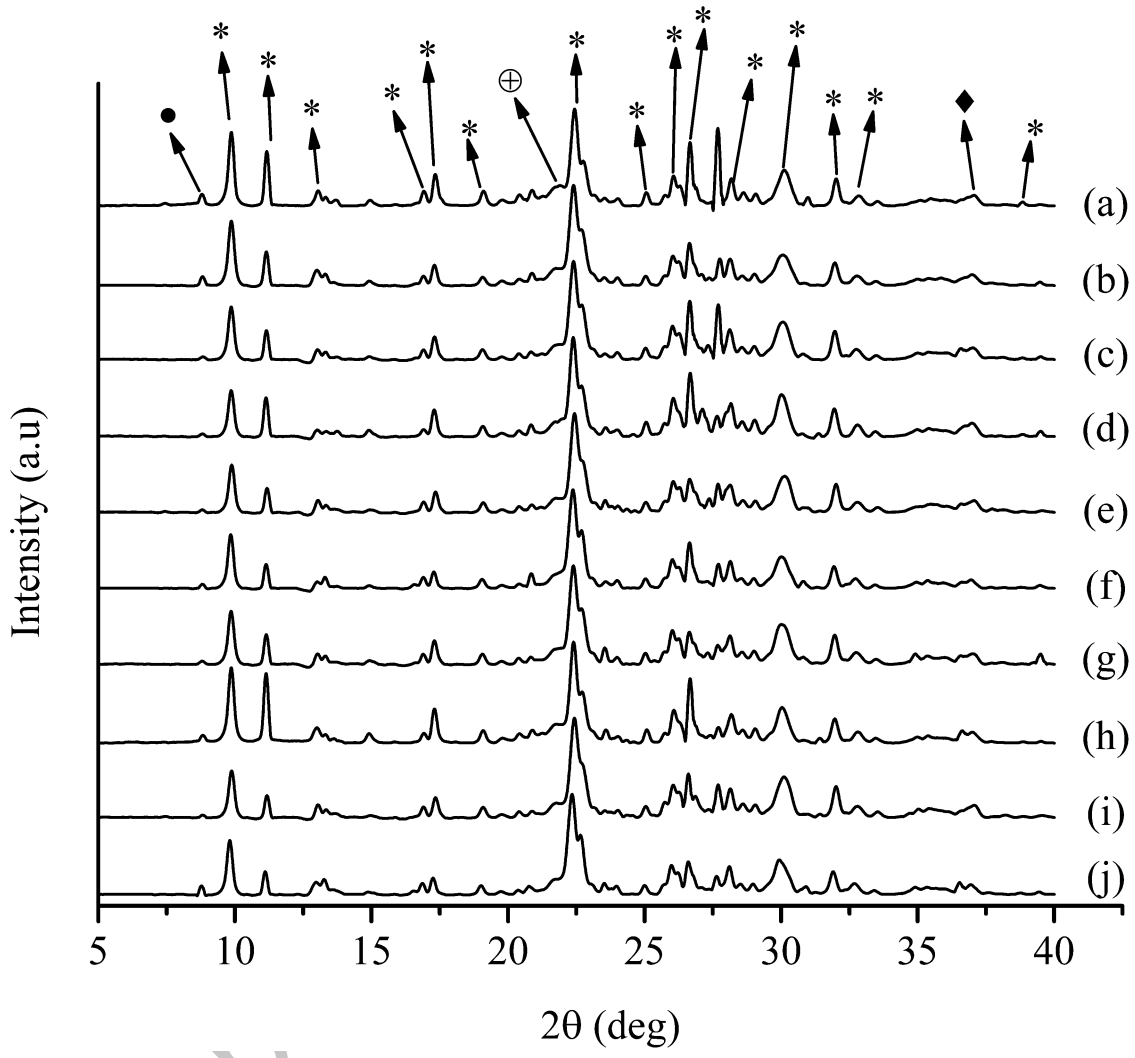

Fig.2 XRD patterns of all specimens. (a): Raw-CLN, (b): Parent-CLN, (c): 0.5-Na-CLN, (d): 0.5-K-CLN, (e): 0.5-Ca-CLN, (f): 0.5-Mg-CLN, (g): 1.0-Na-CLN, (h): 1.0-K-CLN, (i): 1.0-Ca-CLN, (j): 1.0-Mg-CLN (*clinoptilolite, •: illite, ⊕: opal A, ♦: feldspar).

https://doi.org/10.1180/clm.2024.5 Published online by Cambridge University Press

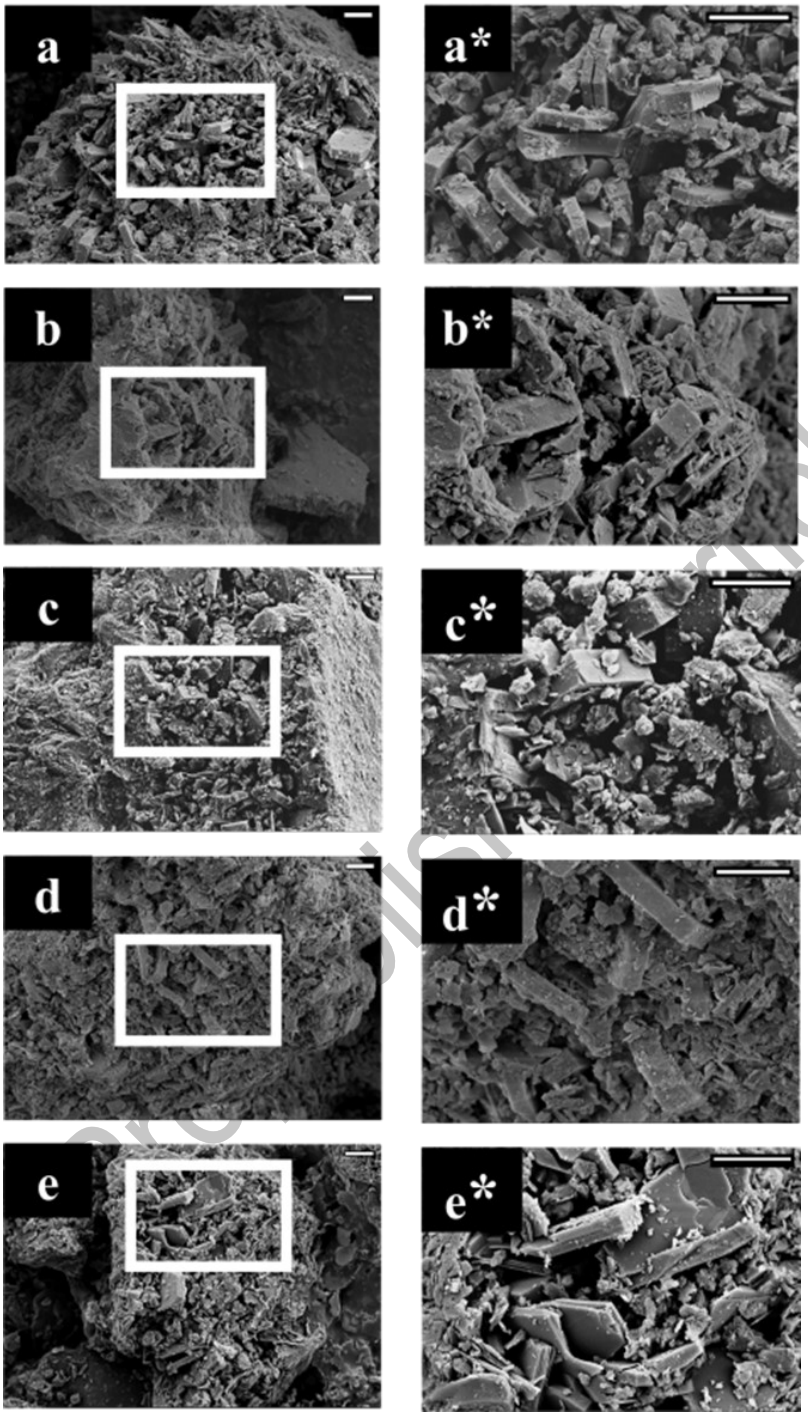

Fig. 3. SEM images of (a) Raw-CLN, (b) 0.5-Na-CLN, (c) 0.5-K-CLN, (d) 0.5-Ca-CLN, (e) 0.5-Mg-CLN at magnification of 5kX. Letters with "*" symbol corresponds to 14kX magnification.

https://doi.org/10.1180/clm.2024.5 Published online by Cambridge University Press

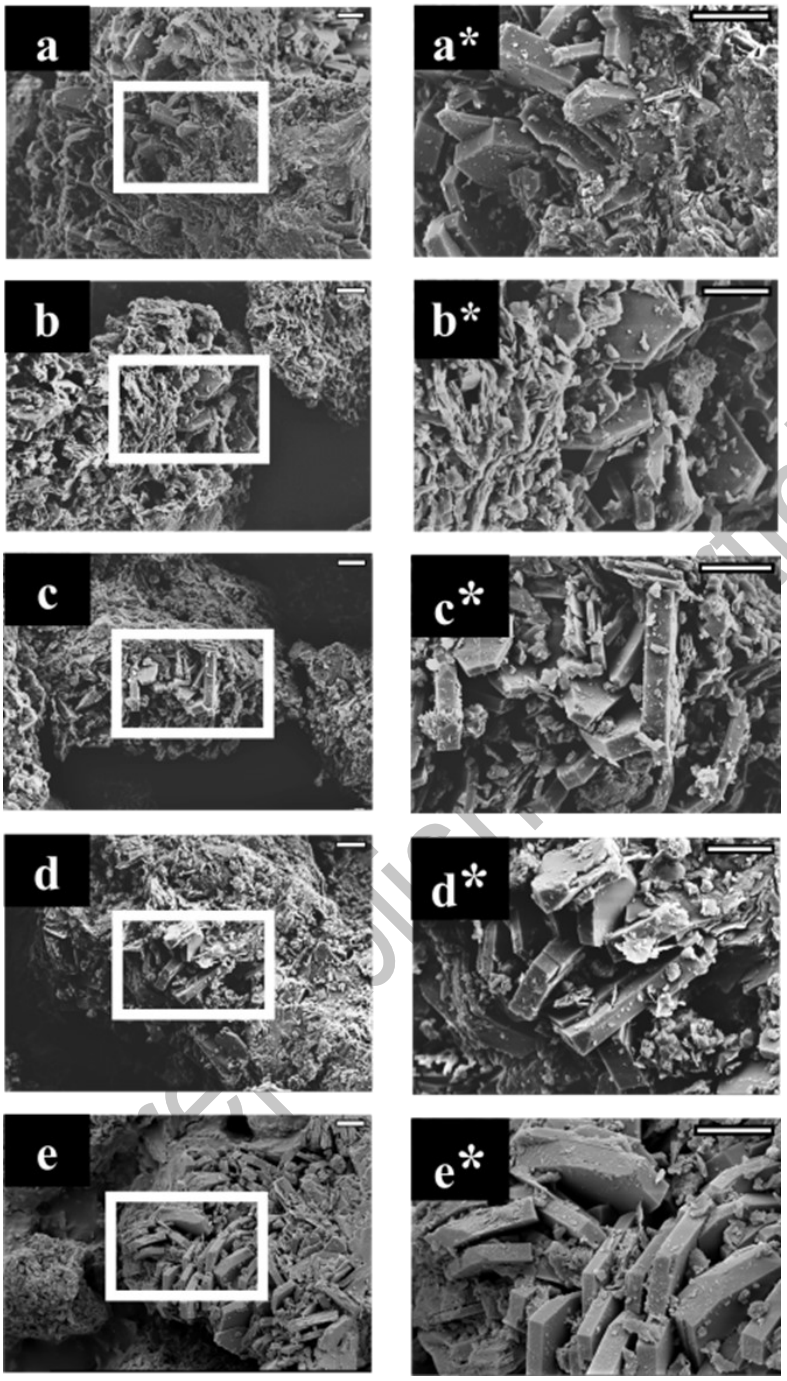

Fig.4. SEM images of (a) Parent-CLN, (b) 1.0-Na-CLN, (c) 1.0-K-CLN, (d) 1.0-Ca-CLN, (e) 1.0-Mg-CLN at magnification of 5kX. Letters with "*" symbol corresponds to 14kX magnification.

https://doi.org/10.1180/clm.2024.5 Published online by Cambridge University Press

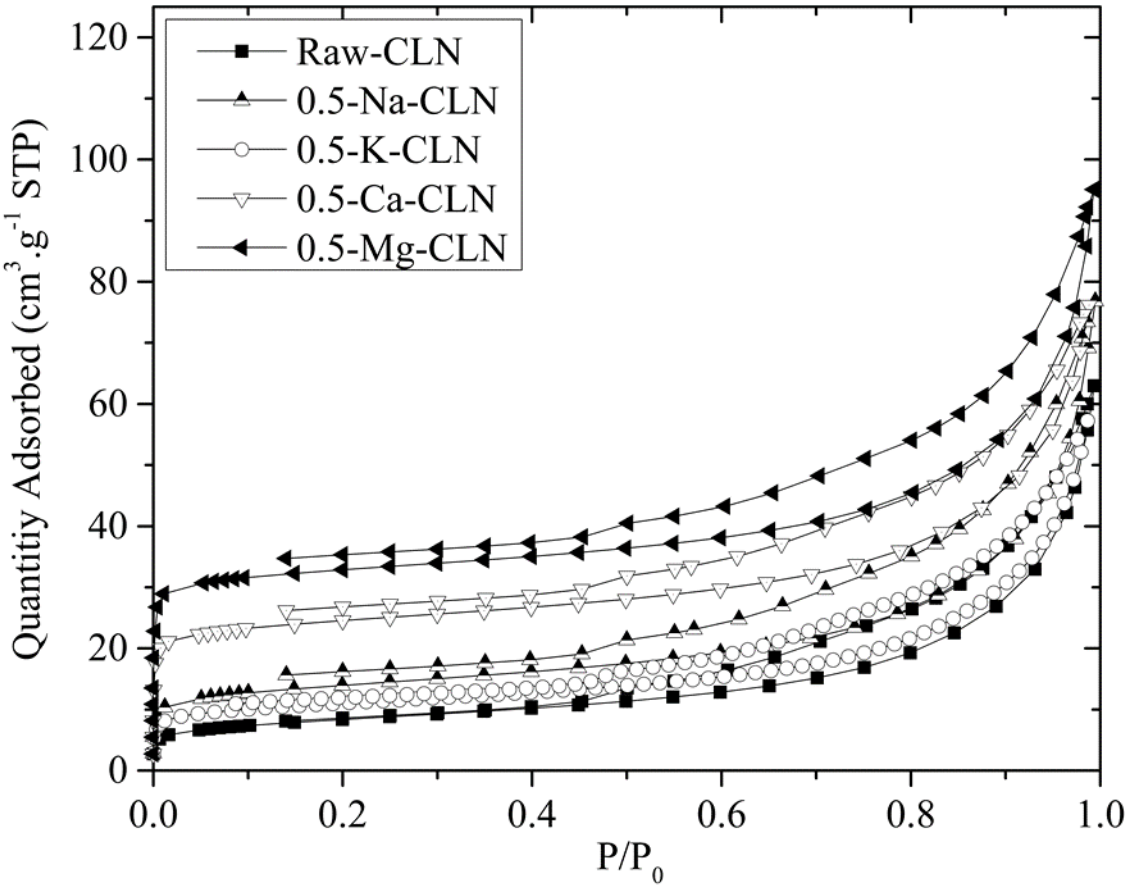

Fig. 5. N_2 adsorption isotherms of raw CLN, 0.5-Na-CLN, 0.5-K-CLN, 0.5-Ca-CLN and 0.5-Mg-CLN samples at 77 K.

https://doi.org/10.1180/clm.2024.5 Published online by Cambridge University Press

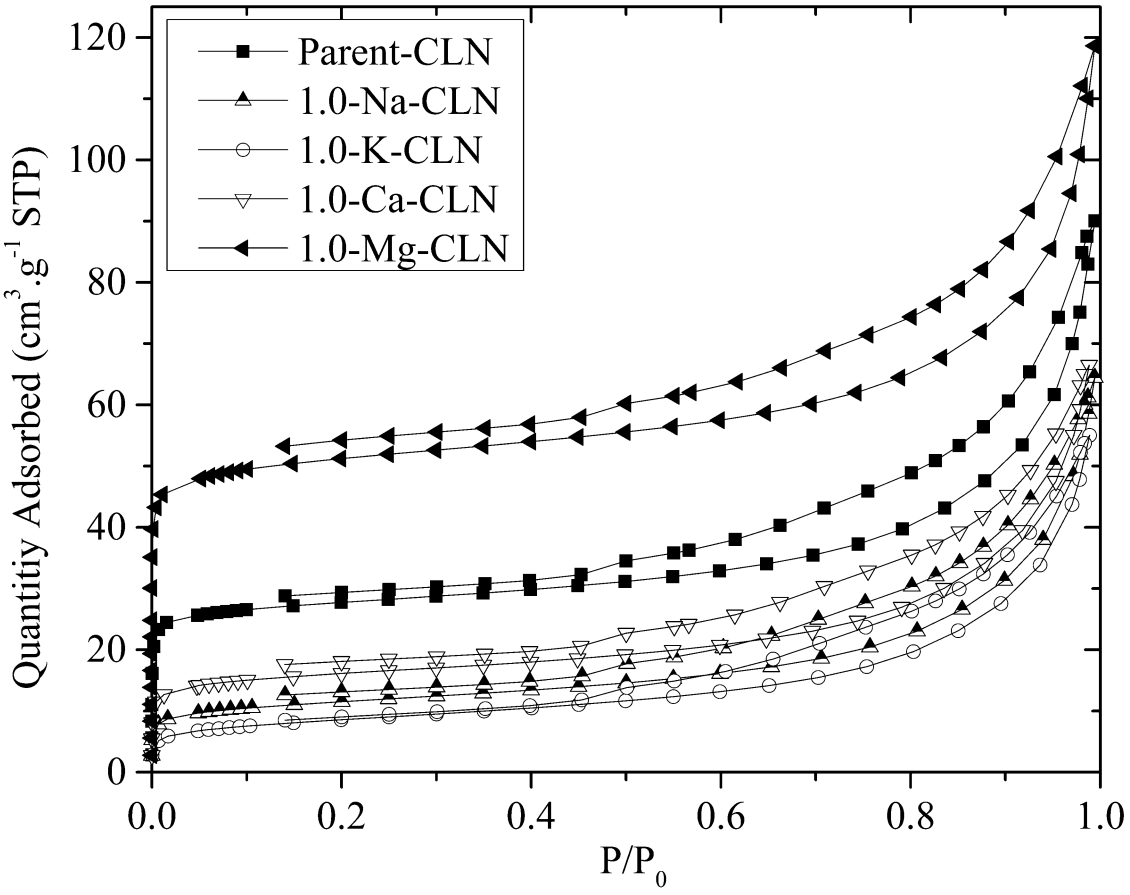

Fig. 6. N_2 adsorption isotherms of parent CLN, 1.0-Na-CLN, 1.0-K-CLN, 1.0-Ca-CLN and 1.0-Mg-CLN samples at 77 K.

https://doi.org/10.1180/clm.2024.5 Published online by Cambridge University Press

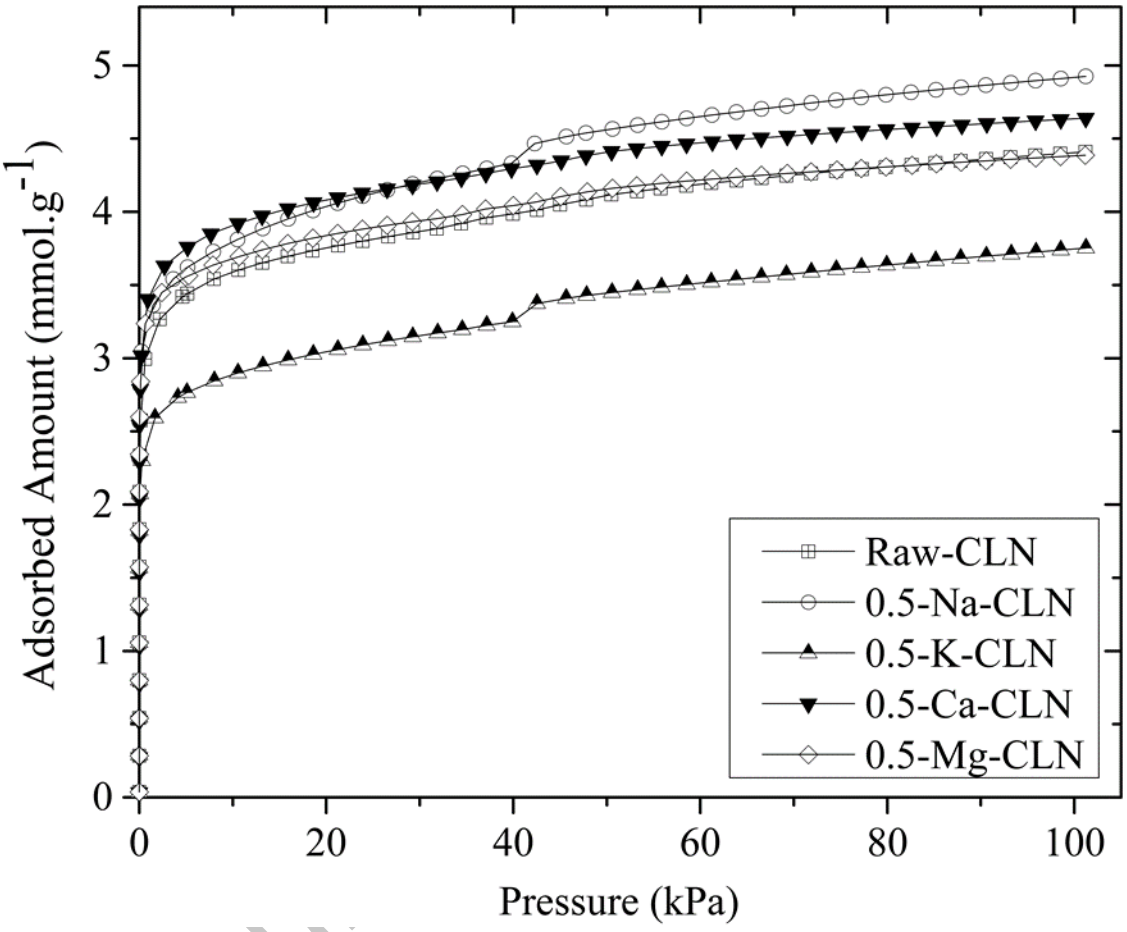

Fig. 7. NH_3 adsorption isotherms of raw CLN, 0.5-Na-CLN, 0.5-K-CLN, 0.5-Ca-CLN and 0.5-Mg-CLN samples at 298 K.

https://doi.org/10.1180/clm.2024.5 Published online by Cambridge University Press

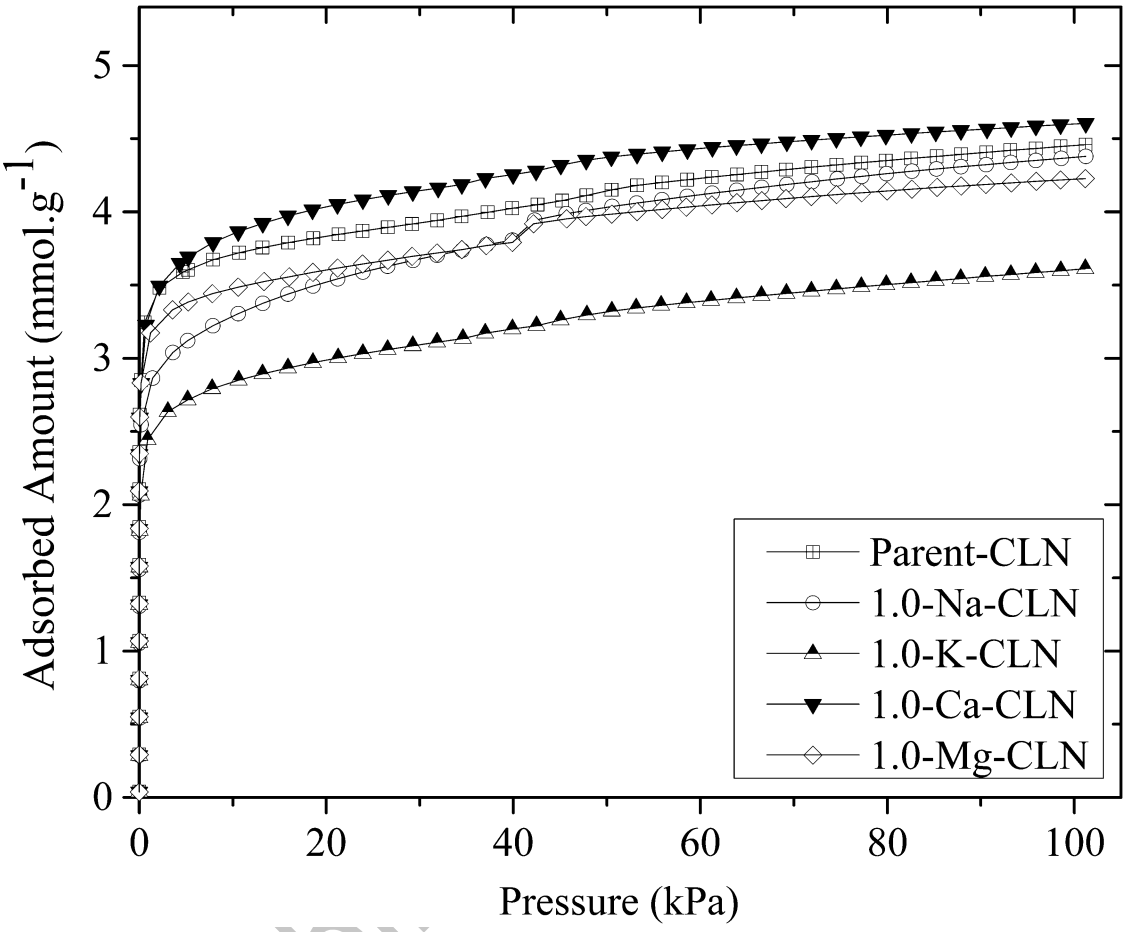

Fig. 8. NH_3 adsorption isotherms of parent CLN, 1.0-Na-CLN, 1.0-K-CLN, 1.0-Ca-CLN and 1.0-Mg-CLN samples at 298 K.

https://doi.org/10.1180/clm.2024.5 Published online by Cambridge University Press

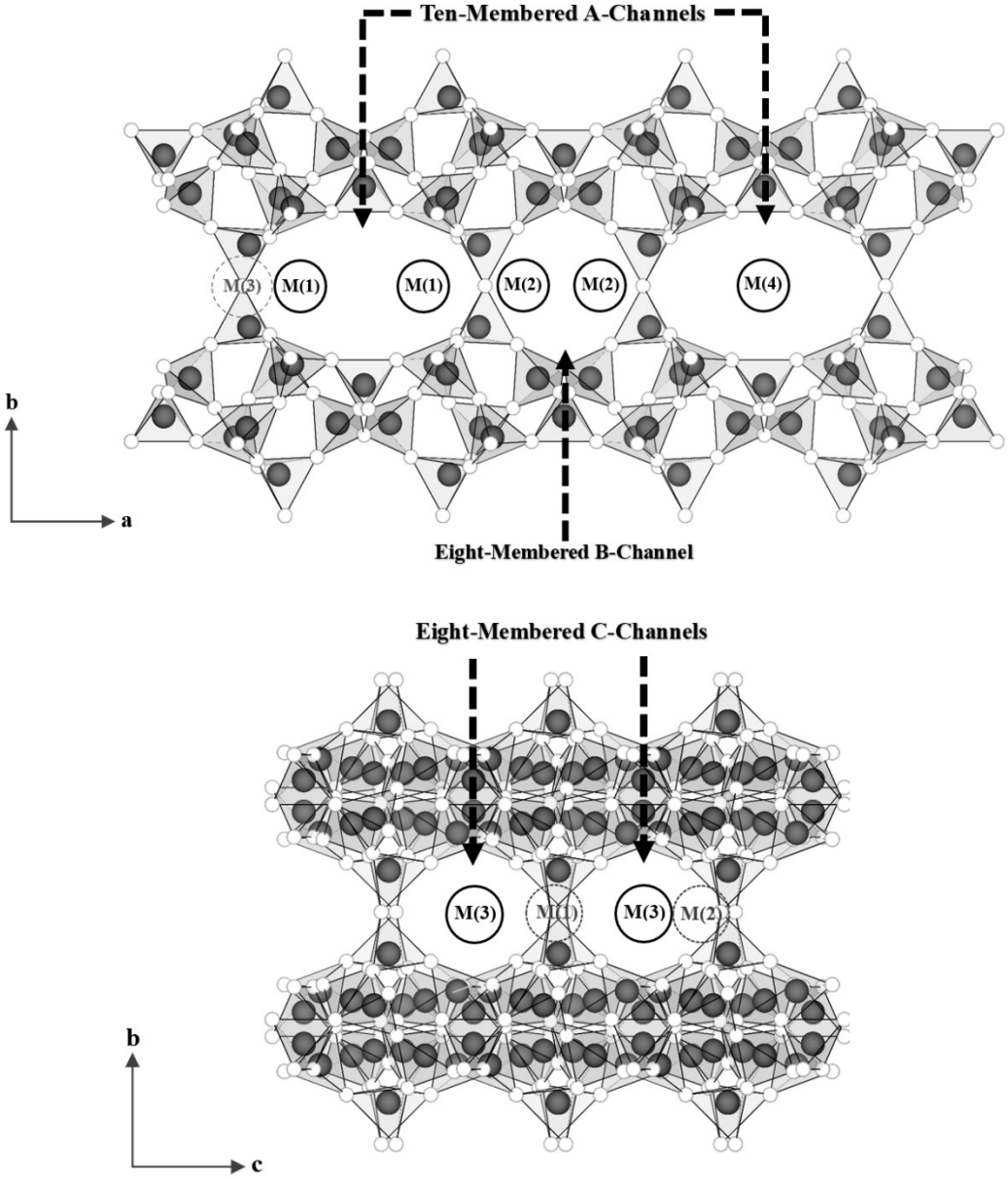

Fig. 9. View of clinoptilolite framework and cation sites along c-axis and a-axis, respectively.

https://doi.org/10.1180/clm.2024.5 Published online by Cambridge University Press

Table 1. Chemical analyses in oxides (%) for raw CLN, parent CLN and its cation exchanged forms.

Chemical analysis (%)	SiO_2	Al_2O_3	Fe_2O_3	MgO	CaO	Na_2O	K_2O	LOI	SiO_2/Al_2O_3
Raw CLN	71.85	12.56	0.82	0.50	1.91	1.04	4.86	6.42	5.7
Parent-CLN	74.68	13.15	0.85	0.22	0.20	0.62	1.83	8.44	5.7
0.5-Na-CLN	74.53	12.91	0.75	0.20	0.22	2.71	1.57	7.07	5.8
1.0-Na CLN	73.96	12.74	0.78	0.24	0.23	3.34	1.64	7.03	5.8
0.5-K-CLN	73.04	12.66	0.76	0.25	0.23	0.62	6.38	5.97	5.8
1.0-K-CLN	73.72	12.49	0.68	0.18	0.23	0.61	6.40	5.68	5.9
0.5-Ca-CLN	73.47	12.05	0.72	0.16	2.10	-	1.59	9.35	6.1
1.0-Ca-CLN	74.53	12.51	0.72	0.15	2.25	0.77	1.69	7.38	5.9
0.5-Mg-CLN	74.58	12.90	0.76	1.09	0.22	0.52	1.70	8.18	5.8
1.0-Mg-CLN	74.75	12.79	0.68	1.12	0.26	0.52	1.83	8.04	5.8

This is a 'preproof' accepted article for Clay Minerals. This version may be subject to change during the production process.
DOI: 10.1180/clm.2024.5

Table 2 Unit-cell parameters and volumes for raw CLN, parent CLN and its cation exchanged forms.

Sample	a (Å)	b (Å)	c (Å)	β (°)	V (Å^3)
Raw CLN	17.775	17.904	7.409	117.20	2097
Parent-CLN	17.759	17.830	7.398	116.97	2088
0.5-Na-CLN	17.789	17.904	7.414	117.13	2101
1.0-Na-CLN	17.754	17.904	7.412	116.91	2101
0.5-K-CLN	17.766	17.924	7.404	116.92	2102
1.0-K-CLN	17.745	17.904	7.402	116.86	2098
0.5-Ca-CLN	17.784	17.868	7.409	117.14	2095
1.0-Ca-CLN	17.770	17.868	7.406	117.10	2093
0.5-Mg-CLN	17.802	17.942	7.411	117.08	2108
1.0-Mg-CLN	17.799	17.998	7.419	117.05	2117

https://doi.org/10.1180/clm.2024.5 Published online by Cambridge University Press

Table 3. N_2 adsorption data of the raw CLN, parent CLN and its cation exchanged forms.

Sample	BET surface area ($m^2.g^{-1}$)	Micropore surface area ($m^2.g^{-1}$)	Micropore volume ($x10^{-2}$ $cm^3.g^{-1}$)
Raw CLN	30.08	8.53	0.35
Parent-CLN	106.93	81.27	3.17
0.5-Na-CLN	49.76	23.70	1.02
0.5-K-CLN	39.98	17.77	0.74
0.5-Ca-CLN	93.15	67.75	2.69
0.5-Mg-CLN	127.03	100.26	3.92
1.0-Na CLN	42.01	20.09	0.82
1.0-K-CLN	30.72	8.46	0.35
1.0-Ca-CLN	60.04	37.05	1.49
1.0-Mg-CLN	198.98	163.36	6.36

Table 4. Comparison of the removal of ammonia by different materials at 298K.

Sample	**Adsorption capacity, (mmol g^{-1})**	**Pressure (kPa)**	**Reference**
Raw CLN	4.41 ± 0.22		present work
Parent-CLN	4.46 ± 0.08		present work
0.5-Na-CLN	4.93 ± 0.12		present work

https://doi.org/10.1180/clm.2024.5 Published online by Cambridge University Press

1.0-Na CLN	4.38 ± 0.00		present work
0.5-K-CLN	3.75 ± 0.19		present work
1.0-K-CLN	3.61 ± 0.00	101	present work
0.5-Ca-CLN	4.64 ± 0.09		present work
1.0-Ca-CLN	4.61 ± 0.04		present work
0.5-Mg-CLN	4.39 ± 0.09		present work
1.0-Mg-CLN	4.23 ± 0.13		present work
Clinoptilolite (USA)	5.90	101	Helminen et al., 2001
Clinoptilolite (Slovakia)	0.71 / (12.2 mg g^{-1})	fixed bed	Ciahotný et al., 2006
MOF-177	12.2	106	[a]Saha & Deng, 2010
13X	9.33	101	Helminen et al., 2001
4A	8.71	101	Helminen et al., 2001
mesoporous carbon	6.39	106	[b]Saha, & Deng, 2010
pentasil dealuminated	2.34	101	Helminen et al., 2001
Cu-MOF-74	3.4	breakthrough	Katz et al., 2016
activated alumina	2.53	108	[c]Saha & Deng, 2010
activated carbon	4.19	101	Helminen et al., 2001
faujasite (dealuminated)	1.77	101	Helminen et al., 2001

https://doi.org/10.1180/clm.2024.5 Published online by Cambridge University Press